A viscous blast-wave model for relativistic heavy-ion collisions

Amaresh Jaiswal

GSI, Helmholtzzentrum für Schwerionenforschung, Planckstrasse 1, D-64291 Darmstadt, Germany

Volker Koch

Lawrence Berkeley National Laboratory, Nuclear Science Division, MS 70R0319, Berkeley, California 94720, USA (Dated: August 25, 2015)

Using a viscosity-based survival scale for geometrical perturbations formed in the early stages of relativistic heavy-ion collisions, we model the radial flow velocity during freeze-out. Subsequently, we employ the Cooper-Frye freeze-out prescription, with first-order viscous corrections to the distribution function, to obtain the transverse momentum distribution of particle yields and flow harmonics. For initial eccentricities, we use the results of Monte Carlo Glauber model. We fix the blast-wave model parameters by fitting the transverse momentum spectra of identified particles at the Large Hadron Collider (LHC) and demonstrate that this leads to a fairly good agreement with transverse momentum distribution of elliptic and triangular flow for various centralities. Within this viscous blast-wave model, we estimate the shear viscosity to entropy density ratio $\eta/s \simeq 0.24$ at the LHC.

PACS numbers: 25.75.-q, 24.10.Nz, 47.75+f

I. INTRODUCTION

High-energy heavy-ion collision experiments at the Relativistic Heavy Ion Collider (RHIC) [1, 2] and the Large Hadron Collider (LHC) [3–5] have conclusively established the formation of a strongly interacting Quark-Gluon Plasma (QGP). The QGP formed in these collisions exhibit strong collective behaviour, and therefore can be studied within the framework of relativistic hydrodynamics. The hydrodynamical analyses of the flow data suggests that the QGP behaves like a nearly perfect fluid with an extremely small shear viscosity to entropy density ratio η/s [6, 7]. Local pressure gradients due to deformations and inhomogeneities in the the initial stages of the collision results in anisotropic fluid velocity. These anisotropies subsequently translate into flow harmonics describing the momentum asymmetry of produced particles [8, 9]. The η/s of the fluid governs the conversion efficiency, which results in a suppression of elliptic flow and higher order flow coefficients [10-23].

Apart from hydrodynamics, the observables pertaining to collective behaviour of QGP can also be studied using the so-called blast-wave model. Using a simple functional form for the phase-space density at kinetic freezeout, Schnedermann et. al. [24] approximated hydrodynamical results with boost-invariant longitudinal flow [25]. They used this blast-wave model to successfully fit the transverse momentum spectra with only two parameters: a kinetic temperature, and a radial flow strength. However, this model was only valid for central collisions at midrapidity. In order to make it applicable for non-central collisions, Huovinen et. al. [26] generalized this model to account for the anisotropies in the transverse flow profile by introducing an additional parameter. This new parameter controlled the difference between the strength of the flow in and out of the reaction plane. This lead to a fairly good fit with the measured elliptical flow as a function of transverse momentum. However, the STAR Collaboration achieved better fits when they generalized the model even further by introducing a fourth parameter to account for the anisotropic shape of the source in coordinate space [27]. Teaney made the first attempt to estimate the effect of viscosity on elliptic flow using a variant of the blast-wave model model [28]. However, the centrality dependence of the fit parameters left the model with little predictive power.

In this paper we generalize the blast-wave model to include viscous effects by employing a viscosity-based survival scale for geometrical anisotropies, formed in the early stages of relativistic heavy-ion collisions, in the parametrization of the radial flow velocity. The present model has five parameters, including η/s , which has to be fitted only for one centrality. In the Cooper-Frye freezeout prescription for particle production, we consider the first-order viscous corrections to the distribution function [28]. In essence, we provide a model which incorporates the important features of viscous hydrodynamic evolution but does not require to do the actual evolution. We use this viscous blast-wave model to obtain the transverse momentum distribution of particle yields and flow harmonics for LHC. The blast-wave model parameters are fixed by fitting the transverse momentum spectra of identified particles. Subsequently, we show that this leads to fairly good agreement with transverse momentum distribution of elliptic and triangular flow for various centralities as well as centrality distribution for integrated flow. We estimate the shear viscosity to entropy density ratio $\eta/s \simeq 0.24$ at the LHC, within the present model.

II. BLAST WAVE MODEL

The blast-wave model has been used extensively to fit experimental data and it provides good description of spectra and elliptic flow observed in relativistic heavy-ion collisions [26–30]. The previously used blast-wave mod-

els employ a simple parametrization for the flow velocity of boost invariant ideal hydrodynamics. The most important feature is the parametrization of the transverse velocity which is assumed to increase linearly with respect to the radius. This parametrization is found to be in agreement with hydro results [31, 32]. This essentially leads to an exponential expansion of the fireball in the transverse direction, hence the term blast-wave. Apart from boost invariance, the model also assumes rotational invariance. In the following, we quickly outline the key features of the blast-wave model.

In order to consider a boost invariant framework, it is easier to work in the Milne co-ordinate system where,

$$\tau = \sqrt{t^2 - z^2},\tag{1}$$

$$\eta_s = \tanh^{-1}(z/t),\tag{2}$$

$$r = \sqrt{x^2 + y^2},\tag{3}$$

$$\varphi = \operatorname{atan2}(y, x). \tag{4}$$

The metric tensor for this co-ordinate system is $g_{\mu\nu} = \text{diag}(1, -\tau^2, -1, -r^2)$. Boost invariance and rotational invariance implies $u^{\varphi} = u^{\eta_s} = 0$, whereas linearly rising transverse velocity flow profile leads to $u^r \sim r$. The blastwave model further assumes that the particle freeze-out happens at a proper time τ_f having a constant temperature T_f and uniform matter distribution, in the transverse plane. In summary, the hydrodynamic fields are parametrized as [28]

$$T = T_f \Theta(R - r), \tag{5}$$

$$u^r = u_0 \frac{r}{P} \Theta(R - r) \tag{6}$$

$$u^{\varphi} = u^{\eta_s} = 0, \tag{7}$$

$$u^{\tau} = \sqrt{1 + (u^r)^2},$$
 (8)

where R is the transverse radius of the fireball at freezeout. The expression for u^{τ} is obtained by requiring that the fluid four-velocity satisfy the condition $u^{\mu}u_{\mu}=1$.

The hadron spectra can be obtained using the Cooper-Frye prescription for particle production [33]

$$\frac{dN}{d^2p_Tdy} = \frac{1}{(2\pi)^3} \int p_\mu d\Sigma^\mu f(x, p),\tag{9}$$

where $d\Sigma_{\mu}$ is the oriented freeze-out hyper-surface and f(x,p) is the phase-space distribution function of the particles at freeze-out. The distribution function can be written in terms of the equilibrium and non-equilibrium parts, $f = f_0 + \delta f$. The equilibrium distribution function is given by

$$f_0 = \frac{1}{\exp(u_\mu p^\mu / T) + a} \ , \tag{10}$$

where a = +1 for baryons and a = -1 mesons.

For small deviations from equilibrium, i.e., $\delta f \ll f_0$, we use the Grad's 14-moment approximation for the non-equilibrium part [34, 35]

$$\delta f = \frac{f_0 \tilde{f}_0}{2(\epsilon + P)T^2} p^{\alpha} p^{\beta} \pi_{\alpha\beta}, \tag{11}$$

where $\tilde{f}_0 = 1 - af_0$ and $\pi_{\alpha\beta}$ is the shear stress tensor. Approximating the shear stress tensor with its first-order relativistic Navier-Stokes expression, $\pi_{\alpha\beta} = 2\eta \nabla_{\langle\alpha} u_{\beta\rangle}$, the expression for the 14-moment approximation reduces to

$$\delta f_1 = \frac{f_0 \tilde{f}_0}{T^3} \left(\frac{\eta}{s}\right) p^{\alpha} p^{\beta} \nabla_{\langle \alpha} u_{\beta \rangle}. \tag{12}$$

Here η is the coefficient of shear viscosity, $s = (\epsilon + P)/T$ is the entropy density and the angular brackets denote traceless symmetric projection orthogonal to the fluid four-velocity [36]. The form of $p^{\alpha}p^{\beta}\nabla_{(\alpha}u_{\beta)}$ in the case of blast-wave model is calculated in Appendix A.

The anisotropic flow is defined as

$$v_n(p_T) \equiv \frac{\int_{-\pi}^{\pi} d\phi \, \cos[n(\phi - \Psi_n)] \, \frac{dN}{dy \, p_t \, dp_T \, d\phi}}{\int_{-\pi}^{\pi} d\phi \, \frac{dN}{dy \, p_t \, dp_T \, d\phi}}, \quad (13)$$

where Ψ_n is the *n*-th harmonic event-plane angle. In the present case, we do not consider event-by-event fluctuations and therefore $\Psi_n = 0$. Up to first order in viscosity [28],

$$v_{n}(p_{T}) = v_{n}^{(0)}(p_{T}) \left(1 - \frac{\int d\phi \frac{dN^{(1)}}{dy \, p_{t} \, dp_{T} \, d\phi}}{\int d\phi \frac{dN^{(0)}}{dy \, p_{t} \, dp_{T} \, d\phi}} \right) + \frac{\int d\phi \, \cos[n(\phi - \Psi_{n})] \frac{dN^{(1)}}{dy \, p_{t} \, dp_{T} \, d\phi}}{\int d\phi \frac{dN^{(0)}}{dy \, p_{t} \, dp_{T} \, d\phi}}, \quad (14)$$

where the superscript '(0)' denotes quantities calculated using the ideal distribution function, Eq. (10), and '(1)' denotes those obtained using the first-order viscous correction, Eq. (12).

III. VISCOUS BLAST-WAVE MODEL

The definition of the participant anisotropies, ε_n , via the Fourier expansion for a single-particle distribution is

$$f(\varphi) = \frac{1}{2\pi} \left[1 + 2 \sum_{n=1}^{\infty} \varepsilon_n \cos[n(\varphi - \psi_n)] \right], \quad (15)$$

where ψ_n are the angles between the x axis and the major axis of the participant distribution. The geometrical anisotropies in the initial particle distribution, ε_n , eventually converts to anisotropies in the radial fluid velocity,

$$u^{r} = u_{0} \frac{r}{R} \left[1 + 2 \sum_{n=1}^{\infty} u_{n} \cos[n(\varphi - \psi_{n})] \right].$$
 (16)

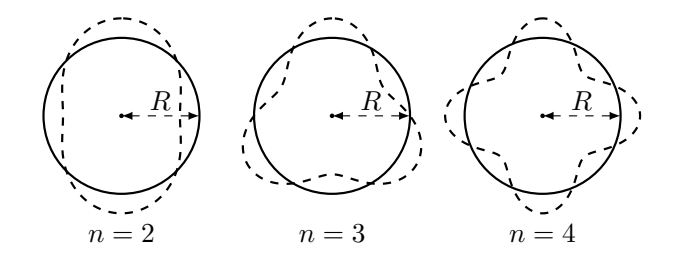


FIG. 1: The harmonics form standing waves on the fireball circumference having radius R at freezeout.

In the following, we determine the conversion efficiency of the initial eccentricity to anisotropy in the radial fluid velocity, u_n/ε_n .

Using the well known dispersion relation for sound in a viscous medium [35],

$$\omega = c_s k + ik^2 \frac{1}{T} \left(\frac{2\eta}{3s} \right), \tag{17}$$

the authors of Ref. [37] introduced a viscosity-based survival scale which all structures formed by point like perturbations should attain at freeze-out. In the above equation, η is the coefficients of shear viscosity and c_s is the speed of sound in the medium. In the present work, we ignore the contribution due to bulk viscosity. Using a plane-wave Fourier ansatz, $\exp(i\omega t - ikx)$, we observe that the amplitudes of the stress tensor harmonics with momentum k are attenuated by a factor

$$\delta T^{\mu\nu}(t,k) = \exp\left[-\left(\frac{2}{3}\frac{\eta}{s}\right)\frac{k^2t}{T}\right]\delta T^{\mu\nu}(0,k), \qquad (18)$$

where we have suppressed the oscillatory pre-factor. We note that the presence of momentum squared in the exponent leads to enhanced effect of viscosity for the higher harmonics. We expect the same qualitative behaviour for the radial flow velocity as will be explained in the following.

First and foremost, we notice that each harmonics is essentially a damped oscillator with wave-vector k. Moreover, throughout the evolution the harmonics form standing waves on the fireball circumference, as shown in Fig. 1, whose amplitude is progressively damped due the viscous effects. Therefore, the fireball circumference is an integer multiple of the wavelength with wave-vector k, i.e.,

$$2\pi R = n\frac{2\pi}{k},\tag{19}$$

where R is the transverse radius of the fireball at freezeout. Hence, at the freeze-out time t_f , the wave amplitude reaction is given by

$$\frac{\delta T^{\mu\nu}|_{t=t_f}}{\delta T^{\mu\nu}|_{t=0}} = \exp\left[-n^2 \left(\frac{2}{3} \frac{\eta}{s}\right) \frac{t_f}{R^2 T_f}\right], \qquad (20)$$

where T_f is the freeze-out temperature.

In absence of viscosity, the initial geometrical perturbations in the fluid will result in the development of radial flow velocity and the conversion efficiency will remain the same for all harmonics. In the case of a viscous medium, however, the conversion efficiency of the initial geometrical perturbation to radial fluid velocity must be proportional to the wave amplitude reaction,

$$\frac{u_n}{\varepsilon_n} = \alpha_0 \exp\left[-n^2 \left(\frac{2}{3} \frac{\eta}{s}\right) \frac{t_f}{R^2 T_f}\right],\tag{21}$$

where α_0 is the constant of proportionality. The sudden stopping of the damped oscillator at the freeze-out time may lead to certain phases due to the oscillatory prefactor. These phases can, in general, lead to secondary peaks in the power spectrum of higher harmonics. However, as no secondary peaks has been observed in the spectrum of relativistic heavy-ion collisions, we will continue to ignore these phase factors.

We emphasize that the acoustic damping should be applied to the hydrodynamic variables, such as the moments of the flow velocity, u_n , rather then to the final state observables such as v_n , as done in Ref. [38]. In Ref. [38], Shuryak and Zahed (S-Z) proposed that the ratio of the initial eccentricity ε_n to the final p_T -integrated v_n should be proportional to the wave amplitude reaction, i.e., the r.h.s. of Eq. (21) should be equal to v_n/ε_n . However, ε_n is the eccentricity in the configuration space whereas v_n is the momentum anisotropy of the particles after freeze-out. The momentum space asymmetries are not hydrodynamic variables and are only affected indirectly via damping. On the other hand, the acoustic damping should be applicable to hydrodynamic variables and it should only capture the viscous effects of the hydrodynamic evolution. This assumption also misses the additional effect of viscosity at freeze-out using the Cooper-Frye formula. Moreover, it does not provide the opportunity to study the p_T dependence of anisotropic flow and hence to estimate the viscosity of the expanding medium.

IV. INITIAL CONDITIONS

In this section, we set-up the initial conditions of the collisions in order to reduce the number of free parameters in the blast-wave model. To this end, we evaluate the parameters corresponding to the initial geometry of the collisions. We also approximate the subsequent transverse expansion of the fireball by using the radial velocity parametrization in the blast-wave model.

We consider the collision of two identical nuclei with mass number A. The radius of each nucleus is given by $R_0 = 1.25 A^{1/3}$ fm and the impact parameter is b, as shown in Fig. 2. The shaded region in Fig. 2 is the overlap zone of the colliding nuclei. We draw a circle of radius r_0 , with its centre coinciding with that of the overlap zone, in such a way that the boundary of the

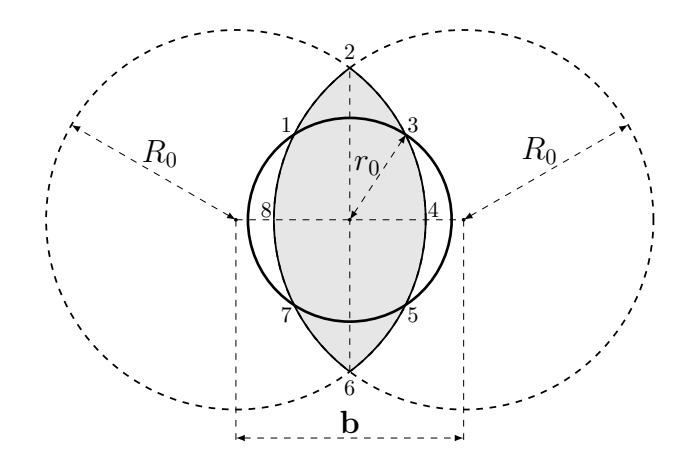


FIG. 2: Initial transverse geometry of the collision of two identical nuclei with radius R_0 and impact parameter b. The shaded region represents the the overlap zone of the colliding nuclei. The circle with radius r_0 is drawn such that it equally divides the boundary of the overlap zone in four parts, i.e., $\widehat{123} = \widehat{345} = \widehat{567} = \widehat{781}$.

overlap zone is equally divided in four parts, i.e., $\widehat{123} = \widehat{345} = \widehat{567} = \widehat{781}$; see Fig. 2. This approximates ε_2 as the second harmonics of initial geometrical fluctuations, analogous to the n=2 case as shown in Fig. 1. The radius r_0 is therefore the initial transverse radius of the expanding fireball and is given by

$$r_0 = \frac{1}{2} \left(b^2 - 2bR_0 \sqrt{2 + \frac{b}{R_0}} + 4R_0^2 \right)^{1/2}, \qquad (22)$$

which reduces to $r_0 = R_0$ for head-on collisions (b = 0). Since ε_2 is the most prominent eccentricity for non-central collisions, all other geometrical eccentricities are treated as boundary perturbations to this circle.

The subsequent transverse expansion of the fireball is obtained by employing the radial velocity parametrization of the blast-wave model. Using the perturbation-free expression for the transverse velocity, Eq. (6), we get

$$u^r \equiv \frac{dr}{d\tau} = u_0 \frac{r}{R} \quad \Rightarrow \quad \int_{r_0}^R \frac{dr}{r} = \int_0^{\tau_f} \frac{u_0}{R} d\tau. \tag{23}$$

After performing the straightforward integration, we obtain a transcendental equation for the freeze-out radius, R,

$$R = r_0 \exp\left(\frac{u_0 \,\tau_f}{R}\right),\tag{24}$$

which can be solved for R given the isotropic expansion velocity u_0 and the freeze-out time τ_0 . In the following, using Bjorken's scaling solution for one-dimensional boost-invariant expansion, we obtain an expression to determine the freeze-out times for non-central collisions once it is fixed for the central one.

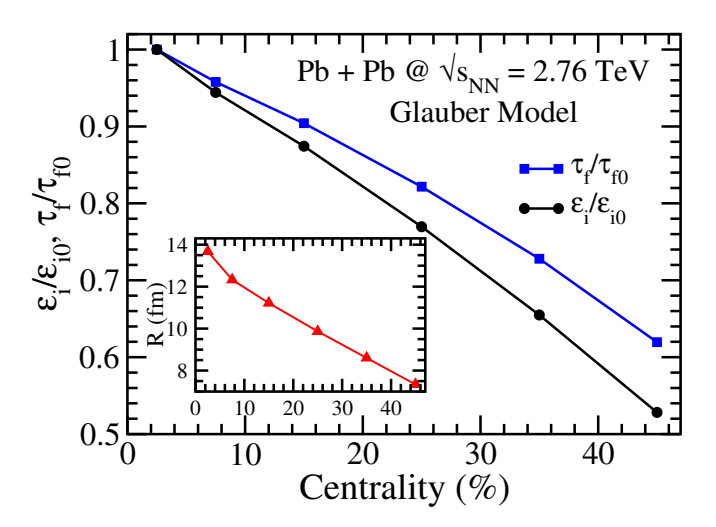


FIG. 3: (Color online) Centrality dependence of the initial energy density ϵ_i and freeze-out time τ_f for Pb+Pb collisions at $\sqrt{s_{NN}} = 2.76$ TeV scaled by the corresponding values in 0-5% central collisions. The inset shows centrality dependence of the freeze-out radius of the fireball R, obtained using Eq. (24).

For the ideal hydrodynamic evolution of relativistic fluid, in the one-dimensional boost-invariant scenario, the evolution of the energy density follows $\epsilon \propto \tau^{-4/3}$. Assuming the initial thermalization time and the final freeze-out energy density (i.e., the freeze-out temperature) to be same for all collisions, we get

$$\tau_f = \tau_{f0} \left(\frac{\epsilon_i}{\epsilon_{i0}}\right)^{3/4}.$$
 (25)

Here τ_{f0} is the freeze-out time for most central collisions, which has to be fixed by fitting the corresponding transverse momentum spectra. The freeze-out times for other centralities can then be obtained using the above equation and therefore they are not free parameters. The ratio ϵ_i/ϵ_{i0} is the initial central energy density scaled by its corresponding value in most central collisions.

Figure 3 shows ϵ_i/ϵ_{i0} for various centralities obtained using the Glauber model calculations [39, 40] in the case of Pb-Pb collisions at $\sqrt{s_{NN}} = 2.76$ TeV at the LHC. We observe that ϵ_i/ϵ_{i0} (and hence the initial temperature) decreases for non-central collisions compared to central ones. Therefore according to Eq. (25), freeze-out happens earlier in peripheral collisions which is also reflected in Fig. 3 for τ_f/τ_{f0} . The inset of Fig. 3 shows the centrality dependence of the freeze-out radius of the fireball R, obtained using Eq. (24). We find a rather large transverse radius of the fireball at freeze-out. Finally, the parameters that we need to fix within the viscous-blast wave model to fit the spectra are the freeze-out temperature T_f , the freeze-out time for central collision τ_{f0} and the unperturbed maximum radial flow velocity u_0 . An interplay of the coefficient of proportionality α_0 in Eq. (21) and η/s will be crucial to reproduce the flow harmonics.

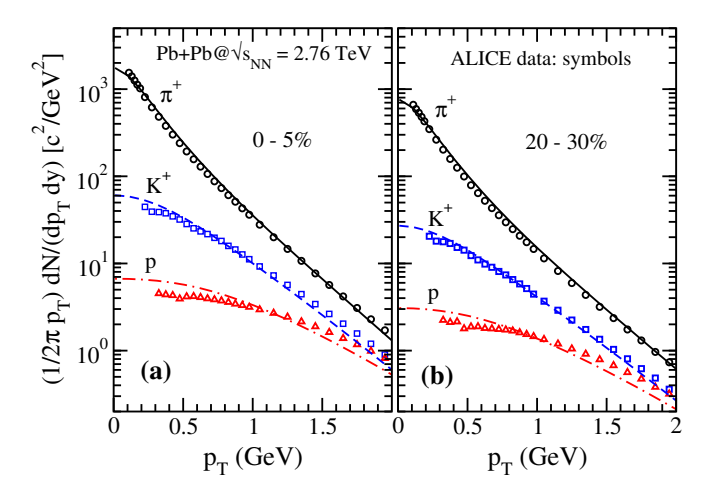


FIG. 4: (Color online) Transverse momentum distribution of particle multiplicities in Pb+Pb collisions at $\sqrt{s_{NN}}=2.76$ TeV. We show results for π^+ , K^+ , and p in two centrality ranges, (a): 0-5% and (b): 20-30%. The symbols represent ALICE data [41] at midrapidity and the lines correspond to viscous blast-wave calculations.

V. RESULTS AND DISCUSSIONS

In this section, we show our results for Pb+Pb collisions at $\sqrt{s_{NN}} = 2.76$ TeV and compare it with experimental data measured at LHC by the ALICE and ATLAS collaborations.

Figure 4 shows the transverse momentum distribution of pions, kaons, and protons spectra for 0-5% and 20-30% central Pb+Pb collisions at $\sqrt{s_{NN}}=2.76$ TeV measured at LHC by the ALICE collaboration (symbols) at midrapidity [41] and calculated using the viscous blastwave model (lines). The results are obtained using root mean square values of eccentricities ε_2 and ε_3 in a Monte-Carlo Glauber model, with a shear viscosity to entropy density ratio $\eta/s = 0.24$. We observe that the spectra for π^+ and K^+ from the viscous blast-wave model are in good overall agreement with the experimental data for a freeze-out temperature of 120 MeV. On the other hand, within the viscous blast-wave model, the proton yield for a freeze-out temperature of 120 MeV is severely underestimated. To obtain an overall fair agreement with the experimental data, the freeze-out temperature for protons is considered to be 135 MeV. The freeze-out time for 0-5% most central collision was found to be 8 fm. For other centralities, the freeze-out time was obtained by using Eq. (25) and results shown in Fig. 3.

Figure 5 shows our results for the $v_n(p_T)$, in comparison with the ATLAS data [4] for various centralities. We find overall fair agreement with the data for elliptic (v_2) and triangular (v_3) flow, at all centralities. This is achieved by choosing a single fixed value $\eta/s = 0.24$ to obtain the required suppression (relative to ideal blastwave results) of v_2 and v_3 , for all centralities. Apart from η/s , flow also depends on the constant of proportionality α_0 appearing in Eq. (21). It controls the conversion

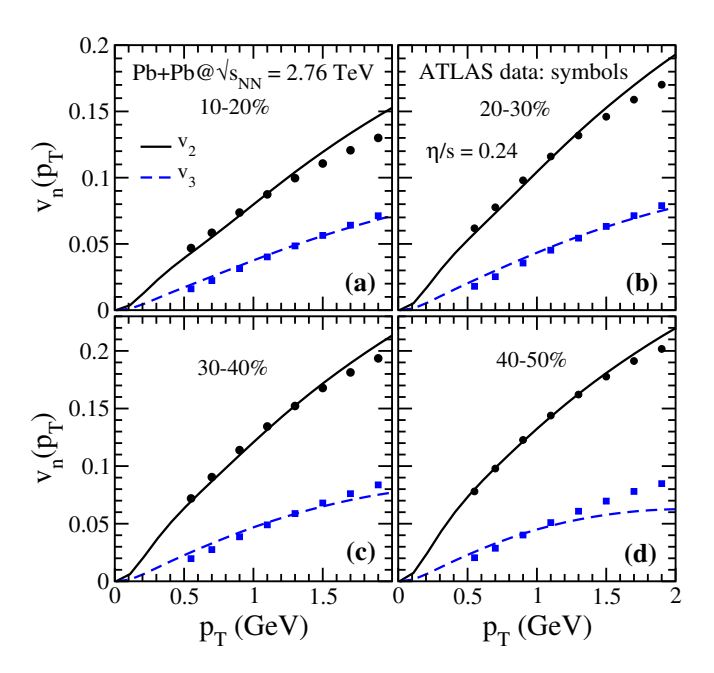


FIG. 5: (Color online) Transverse momentum dependence of the anisotropic flow coefficients $v_n(p_T)$ of charged hadrons, for n=2 and 3, calculated at various centralities in Pb+Pb collisions at $\sqrt{s_{NN}}=2.76$ TeV in the viscous blast-wave model (lines) with $\eta/s=0.24$ as compared to the ATLAS data [4] (symbols).

efficiency of the initial eccentricity to final fluid velocity. We consider the initial eccentricity ε_n to be the rms values of the eccentricities obtained in the MC-Glauber model, as given in Ref. [42]. A large value of α_0 means larger conversion of eccentricity leading to increased flow velocity and hence higher v_2 and v_3 . On the other hand, as is well known, an increase in η/s leads to suppression of v_2 and v_3 . Large (small) value of α_0 can be compensated by choosing a higher (lower) value of η/s up to a certain extent. However, beyond a certain range of η/s , the relative behaviour of v_2 and v_3 is destroyed.

In order to match the elliptic and triangular flow data, we find the most suitable parameter values for $\alpha_0 = 0.4$ and $\eta/s = 0.24$. Moreover, we find that v_n is insensitive to a for transverse velocity of the form $v^r \sim (r/R)^a$. This may be attributed to the fact that the exponent a controls the rate of isotropic transverse expansion. The anisotropic flow originates from the initial eccentricity which translates into final flow. Therefore v_n is sensitive to u_n which depends on α_0 and η/s , as is apparent from Eq. (21). On the other hand, it should be noted that the slope of the particle spectra is sensitive to the exponent a and could be tuned to get a better fit with the experimental data. However, in the present work, we are interested in the anisotropic flow and therefore we set a = 1 and do not fit it to match the particle spectra.

In Fig. 6(a), p_T -integrated values of v_2 and v_3 obtained from the viscous blast-wave model are compared with ALICE data [3], as a function of centrality. We observe that using the same constant $\eta/s = 0.24$ for all central-

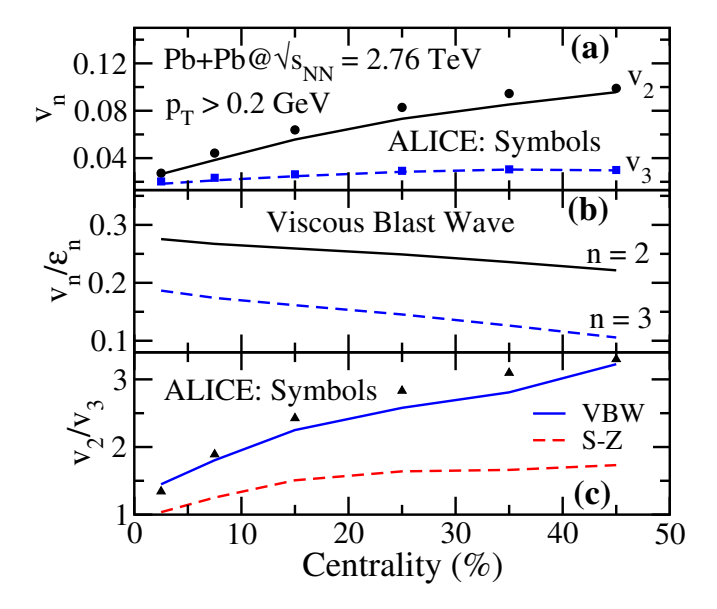


FIG. 6: (Color online) (a): Centrality dependence of the p_T integrated anisotropic flow coefficients v_n of charged hadrons in Pb+Pb collisions at $\sqrt{s_{NN}}=2.76$ TeV calculated in the viscous blast-wave model (lines) with $\eta/s=0.24$, as compared to ALICE data [3] (symbols). (b): Centrality dependence of the ratio v_n/ε_n in the viscous blast-wave model where ε_n is the rms values of the eccentricities obtained in the MC-Glauber model [42]. In panels (a) and (b), we show results for n=2 and 3. (c): Centrality dependence of the ratio v_2/v_3 for ALICE data (symbols), using the viscous blast-wave model (solid line) and from the Shuryak-Zahed estimate (dashed line).

ities, the model shows a good agreement with the data. Since v_2 is driven mostly by the initial spatial anisotropy, it exhibits a strong centrality dependence compared to v_3 . Figure 6(b) shows the conversion efficiency of the initial spatial anisotropy into the final momentum anisotropy. A linear relation between v_n and ε_n , as observed in some hydrodynamic calculations [23], is not obtained within the viscous blast-wave model presented here. On the other hand, in view of the non-linear nature of the hydrodynamic equations a linear relation between v_n and ε_n is not obvious. Indeed other calculations [43] as well as a recent analysis of the LHC data [44] also result in a similar centrality dependence as obtained in our analysis In Fig. 6(c), we show the ratio v_2/v_3 as a function of centrality for the ALICE data (symbols), the present viscous blast-wave model (blue solid line) and the estimate due to Shuryak and Zahed (red dashed line). We see that the viscous blast-wave model provides a better agreement with ALICE data compared to the S-Z estimate. However, we should keep in mind that the freezeout parameters used in the S-Z estimate is the same as that of the viscous blast-wave fit values.

VI. CONCLUSIONS AND OUTLOOK

In this paper we have generalized the blast-wave model to include viscous effects by employing a viscosity-based survival scale for geometrical anisotropies formed in the early stages of relativistic heavy-ion collisions. This viscous damping is introduced in the parametrization of the radial flow velocity. The viscous blast wave model presented here involved five parameters, including η/s , which has to be fitted for only one centrality. This model therefore incorporates the important features of viscous hydrodynamic evolution but does not require to do the actual evolution. We have used this viscous blastwave model to obtain the transverse momentum distribution of particle yields and anisotropic flow harmonics for LHC. The blast-wave model parameters were fixed by fitting the transverse momentum spectra of identified particles. We demonstrated that a fairly good agreement was achieved for transverse momentum distribution of elliptic and triangular flow for various centralities as well as centrality distribution for the integrated flow. Within the present model, we estimated the shear viscosity to entropy density ratio $\eta/s \simeq 0.24$ at the LHC.

One of the drawbacks of the present model is that we have employed root mean squared eccentricity over number of events, which is analogous to "single shot" hydrodynamic evolution. On the plus side, the present model could also be implemented on an event-by-event basis. Another difficulty that we encountered was that in order to fit the proton spectra, we had to consider a different freeze-out temperature (135 MeV) compared to that for pions and Kaons (120 MeV). This problem could be addressed by parametrizing the transverse velocity in the form $v^r \sim (r/R)^a$ and fitting a for different particle species, separately. We leave these problems for a future work.

Acknowledgments

A.J. acknowledges useful discussions with Subrata Pal, Krzysztof Redlich, Edward Shuryak and Derek Teaney. A.J. thanks Victor Roy for helpful comments and providing data from Glauber model. A.J. was supported by the Frankfurt Institute for Advanced Studies (FIAS), Germany.

Appendix A: Viscous stress tensor

In this Appendix, we calculate the viscous tensor $\nabla_{\langle\alpha}u_{\beta\rangle}$ and therefore obtain the viscous corrections to the distribution function at freeze-out. We work in Milne co-ordinate system, Eqs. (1)-(4) with the metric tensor $g_{\mu\nu}={\rm diag}(1,-\tau^2,-1,-r^2)$. Therefore, the inverse metric tensor is $g^{\mu\nu}={\rm diag}(1,-1/\tau^2,-1,-1/r^2)$, its determinant g is $\sqrt{-g}=\tau r$ and the non-vanishing Christoffel symbols are $\Gamma^{\tau}_{\eta_{\pi}\eta_{s}}=\tau$, $\Gamma^{\eta_{\pi}}_{\eta_{\pi}}=1/\tau$, $\Gamma^{\tau}_{\varphi\varphi}=-r$, and

 $\Gamma_{r\varphi}^{\varphi} = 1/r$. Using the parametrization of the fluid velocity given in Eqs. (6)-(8), we get

$$\Delta^{r\varphi} = 0, \quad \Delta^{\varphi\varphi} = -\frac{1}{r^2}, \quad \Delta^{rr} = -1 - (u^r)^2, \quad (A1)$$

$$\partial_r u^r = \frac{u^r}{r}, \quad \partial_\varphi u^r = -\frac{2u_0 r}{R} \sum_{n=1}^\infty n \, u_n \sin[n(\varphi - \psi_n)]. \quad (A2)$$

where $\Delta^{\mu\nu} \equiv g^{\mu\nu} - u^{\mu}u^{\nu}$ is the projection operator orthogonal to the fluid four-velocity.

To fix the time derivatives of the fluid velocity, we assume that if the particles are freezing-out, they are free streaming, which means that $Du^{\mu}=0$. Here $D\equiv u^{\mu}d_{\mu}$ is the co-moving derivative and d_{μ} is the covariant derivative. With this prescription, we have

$$\begin{split} &\partial_{\tau}u^{\varphi}=0,\\ &\partial_{\tau}u^{r}=-v\,\partial_{r}u^{r}=-\frac{(u^{r})^{2}}{ru^{\tau}},\\ &\partial_{\tau}u^{\tau}=v\,\partial_{\tau}u^{r}=-\frac{(u^{r})^{3}}{r(u^{\tau})^{2}} \end{split} \tag{A3}$$

where $v = u^r/u^\tau$ is the radial velocity. The expansion scalar is given by

$$\frac{1}{\sqrt{-g}}\partial_{\mu}(\sqrt{-g}u^{\mu}) = \frac{u^{\tau}}{\tau} + \frac{u^{r}}{r} + \partial_{\varphi}u^{\varphi} + \partial_{r}u^{r} + \partial_{\tau}u^{\tau},$$

$$= \frac{u^{\tau}}{\tau} + 2\frac{u^{r}}{r} - \frac{(u^{r})^{3}}{r(u^{\tau})^{2}}.$$
(A4)

Assuming boost invariance, the spatial components of the viscous tensor are given by

$$r\nabla^{\langle r}u^{\varphi\rangle} = -\frac{r}{2}\partial_{r}u^{\varphi} - \frac{1}{2r}\partial_{\varphi}u^{r} - \frac{r}{2}u^{r}Du^{\varphi} - \frac{r}{2}u^{\varphi}Du^{r}$$
$$-\frac{1}{3}r\Delta^{r\varphi}\frac{1}{\sqrt{-g}}\partial_{\mu}(\sqrt{-g}u^{\mu})$$
$$= \frac{u_{0}}{R}\sum_{n=1}^{\infty}nu_{n}\sin[n(\varphi - \psi_{n})], \tag{A5}$$

$$\begin{split} r^2 \nabla^{\langle \varphi} u^{\varphi \rangle} &= - \, \partial_{\varphi} u^{\varphi} - \frac{u^r}{r} - r^2 u^{\varphi} D u^{\varphi} \\ &- \frac{1}{3} r^2 \Delta^{\varphi \varphi} \frac{1}{\sqrt{-g}} \partial_{\mu} (\sqrt{-g} u^{\mu}) \\ &= \frac{1}{3} \left[\frac{u^{\tau}}{\tau} - \frac{u^r}{r} - \frac{(u^r)^3}{r(u^{\tau})^2} \right] \,, \end{split} \tag{A6}$$

$$\nabla^{\langle r} u^{r \rangle} = -\partial_r u^r - u^r D u^r - \frac{1}{3} \Delta^{rr} \frac{1}{\sqrt{-g}} \partial_\mu (\sqrt{-g} u^\mu)$$
$$= \frac{1}{3} \left[\frac{(u^\tau)^3}{\tau} - \frac{u^r}{r} + \frac{(u^r)^3}{r} \right], \tag{A7}$$

where we have used the fact that $(u^{\tau})^2 = 1 + (u^r)^2$.

$$\begin{split} \tau^2 \nabla^{\langle \eta_s} u^{\eta_s \rangle} &= -\frac{u^{\tau}}{\tau} + \frac{1}{3} \frac{1}{\sqrt{-g}} \partial_{\mu} (\sqrt{-g} u^{\mu}) \\ &= \frac{1}{3} \left[2 \frac{u^r}{r} - 2 \frac{u^{\tau}}{\tau} - \frac{(u^r)^3}{r(u^{\tau})^2} \right] \,, \end{split} \tag{A8}$$

$$\nabla^{\langle r} u^{\eta_s \rangle} = \nabla^{\langle \varphi} u^{\eta_s \rangle} = 0. \tag{A9}$$

To obtain the temporal components of the viscous stress energy tensor, we use the Landau frame condition, $\nabla^{\langle \alpha} u^{\beta \rangle} u_{\beta} = 0$.

$$\begin{split} \nabla^{\langle \tau} u^{\tau \rangle} u_{\tau} + \nabla^{\langle \tau} u^{r \rangle} u_{r} &= 0 \quad \Rightarrow \quad \nabla^{\langle \tau} u^{\tau \rangle} = v \nabla^{\langle \tau} u^{r \rangle}, \\ (\text{A}10) \\ \nabla^{\langle \eta_{s}} u^{\tau \rangle} u_{\tau} + \nabla^{\langle \eta_{s}} u^{r \rangle} u_{r} &= 0 \quad \Rightarrow \quad \nabla^{\langle \tau} u^{\eta_{s} \rangle} &= 0, \quad (\text{A}11) \\ \nabla^{\langle r} u^{\tau \rangle} u_{\tau} + \nabla^{\langle r} u^{r \rangle} u_{r} &= 0 \quad \Rightarrow \quad \nabla^{\langle \tau} u^{r \rangle} &= v \nabla^{\langle r} u^{r \rangle}, \\ (\text{A}12) \\ \nabla^{\langle \varphi} u^{\tau \rangle} u_{\tau} + \nabla^{\langle \varphi} u^{r \rangle} u_{r} &= 0 \quad \Rightarrow \quad \nabla^{\langle \tau} u^{\varphi \rangle} &= v \nabla^{\langle r} u^{\varphi \rangle}. \end{split}$$

Therefore, from Eqs. (A10) and (A12), we see that

$$\nabla^{\langle \tau} u^{\tau \rangle} = v \nabla^{\langle \tau} u^{r \rangle} = v^2 \nabla^{\langle \tau} u^{r \rangle}$$

$$= \frac{1}{3} \left[\frac{(u^r)^2 u^{\tau}}{\tau} - \frac{(u^r)^3}{r(u^{\tau})^2} + \frac{(u^r)^5}{r(u^{\tau})^2} \right].$$
 (A14)

Next, in order to verify our algebra, we confirm that the viscous stress tensor is traceless, i.e., $g_{\mu\nu}\nabla^{\langle\mu}u^{\nu\rangle}=0$. Using Eqs. (A6), (A7), (A8) and (A14)

$$g_{\mu\nu} \nabla^{\langle \mu} u^{\nu \rangle} = \nabla^{\langle \tau} u^{\tau \rangle} - \tau^2 \nabla^{\langle \eta_s} u^{\eta_s \rangle} - \nabla^{\langle \tau} u^{\tau \rangle} - r^2 \nabla^{\langle \varphi} u^{\varphi \rangle}$$

$$= \frac{1}{3} \left[\frac{(u^r)^2 u^\tau}{\tau} - \frac{(u^r)^3}{r(u^\tau)^2} + \frac{(u^r)^5}{r(u^\tau)^2} \right]$$

$$- \frac{1}{3} \left[2 \frac{u^r}{r} - 2 \frac{u^\tau}{\tau} - \frac{(u^r)^3}{r(u^\tau)^2} \right]$$

$$- \frac{1}{3} \left[\frac{(u^\tau)^3}{\tau} - \frac{u^r}{r} + \frac{(u^r)^3}{r} \right]$$

$$- \frac{1}{3} \left[\frac{u^\tau}{\tau} - \frac{u^r}{r} - \frac{(u^r)^3}{r(u^\tau)^2} \right]$$

$$= 0. \tag{A15}$$

For a particle at the space-time point $(\tau, \eta_s, r, \varphi)$ with the four momentum $p^{\mu} = (E, p^x, p^y, p^z) = (m_T \cosh y, p_T \cos \varphi_p, p_T \sin \varphi_p, m_T \sinh y)$, we get

$$p^{\tau} = m_{T} \cosh(y - \eta_{s}) \Rightarrow p_{\tau} = m_{T} \cosh(y - \eta_{s}),$$

$$\tau p^{\eta_{s}} = m_{T} \sinh(y - \eta_{s}) \Rightarrow p_{\eta_{s}} = -\tau m_{T} \sinh(y - \eta_{s}),$$

$$p^{r} = p_{T} \cos(\varphi_{p} - \varphi) \Rightarrow p_{r} = -p_{T} \cos(\varphi_{p} - \varphi),$$

$$r p^{\varphi} = p_{T} \sin(\varphi_{p} - \varphi) \Rightarrow p_{\varphi} = -r p_{T} \sin(\varphi_{p} - \varphi).$$
(A16)

The oriented freeze-out hyper-surface is $d\Sigma_{\mu} = (\tau d\eta_s \, r dr \, d\varphi, \, 0, \, 0, \, 0)$, and therefore the integration measure is given by

$$p^{\mu}d\Sigma_{\mu} = m_T \cosh(y - \eta_s) \tau d\eta_s \, r dr \, d\varphi. \tag{A17}$$

The viscous correction to the equilibrium distribution function is proportional to

$$\begin{split} p_{\mu}p_{\nu}\nabla^{\langle\mu}u^{\nu\rangle} &= p_{\tau}^{2}\nabla^{\langle\tau}u^{\tau\rangle} + p_{\eta_{s}}^{2}\nabla^{\langle\eta_{s}}u^{\eta_{s}\rangle} + p_{r}^{2}\nabla^{\langle r}u^{r\rangle} \\ &+ p_{\varphi}^{2}\nabla^{\langle\varphi}u^{\varphi\rangle} + 2p_{\tau}p_{r}\nabla^{\langle\tau}u^{r\rangle} + 2p_{r}p_{\varphi}\nabla^{\langle r}u^{\varphi\rangle} \\ &+ 2p_{\tau}p_{\varphi}\nabla^{\langle\tau}u^{\varphi\rangle}. \end{split} \tag{A18}$$

The final form of $f = f_0 + \delta f$ obtained from Eq. (12) using

the above equation is required to evaluate the spectra given by

$$\frac{d^2N}{d^2p_T \, dy} = \frac{1}{(2\pi)^3} \int_0^R dr \int_0^{2\pi} d\varphi \int_{-\infty}^{\infty} d\eta_s \, m_T \cosh(y - \eta_s) f.$$
(A19)

- J. Adams *et al.* [STAR Collaboration], Nucl. Phys. A 757, 102 (2005).
- [2] K. Adcox et al. [PHENIX Collaboration], Nucl. Phys. A 757, 184 (2005).
- [3] K. Aamodt *et al.* [ALICE Collaboration], Phys. Rev. Lett. **107**, 032301 (2011).
- [4] G. Aad et al. [ATLAS Collaboration], Phys. Rev. C 86, 014907 (2012).
- [5] S. Chatrchyan *et al.* [CMS Collaboration], Phys. Rev. C 89, 044906 (2014).
- [6] P. Romatschke and U. Romatschke, Phys. Rev. Lett. 99, 172301 (2007).
- [7] H. Song and U. W. Heinz, Phys. Rev. C 77, 064901 (2008).
- [8] U. Heinz and R. Snellings, Ann. Rev. Nucl. Part. Sci. 63, 123 (2013).
- [9] C. Gale, S. Jeon and B. Schenke, Int. J. Mod. Phys. A 28, 1340011 (2013).
- [10] M. Luzum and P. Romatschke, Phys. Rev. C 78, 034915 (2008). [Erratum *ibid*. C 79, 039903(E) (2009)].
- [11] H. Song and U. Heinz, Phys. Lett. B658, 279 (2008); Phys. Rev. C 78, 024902 (2008);
- [12] J. Steinheimer, M. Bleicher, H. Petersen, S. Schramm, H. Stocker and D. Zschiesche, Phys. Rev. C 77, 034901 (2008).
- [13] K. Dusling and D. Teaney, Phys. Rev. C 77, 034905 (2008).
- [14] D. Molnar and P. Huovinen, J. Phys. G 35, 104125 (2008).
- [15] P. Bozek, Phys. Rev. C 81, 034909 (2010).
- [16] A. K. Chaudhuri, J. Phys. G 37, 075011 (2010).
- [17] Z. Xu, C. Greiner, and H. Stöcker, Phys. Rev. Lett. 101, 082302 (2008).
- [18] H. Holopainen, H. Niemi and K. J. Eskola, Phys. Rev. C 83, 034901 (2011).
- [19] Z. Qiu and U. W. Heinz, Phys. Rev. C 84, 024911 (2011).
- [20] H. Song, S. A. Bass, U. Heinz, T. Hirano and C. Shen, Phys. Rev. Lett. 106, 192301 (2011) [Erratum-ibid. 109, 139904 (2012)].
- [21] B. Schenke, S. Jeon and C. Gale, Phys. Rev. Lett. 106, 042301 (2011); Phys. Rev. C 85, 024901 (2012).

- [22] Z. Qiu, C. Shen and U. Heinz, Phys. Lett. B 707, 151 (2012).
- [23] R. S. Bhalerao, A. Jaiswal and S. Pal, Phys. Rev. C 92, 014903 (2015).
- [24] E. Schnedermann, J. Sollfrank and U. W. Heinz, Phys. Rev. C 48, 2462 (1993).
- [25] J. D. Bjorken, Phys. Rev. D 27, 140 (1983).
- [26] P. Huovinen, P. F. Kolb, U. W. Heinz, P. V. Ruuskanen and S. A. Voloshin, Phys. Lett. B 503, 58 (2001).
- [27] C. Adler et al. [STAR Collaboration], Phys. Rev. Lett. 87, 182301 (2001).
- [28] D. Teaney, Phys. Rev. C 68, 034913 (2003).
- [29] Z. Tang, Y. Xu, L. Ruan, G. van Buren, F. Wang and Z. Xu, Phys. Rev. C 79, 051901 (2009).
- [30] X. Sun, H. Masui, A. M. Poskanzer and A. Schmah, Phys. Rev. C 91, 024903 (2015).
- [31] D. Teaney, J. Lauret and E. V. Shuryak, nucl-th/0110037.
- [32] M. Habich, J. L. Nagle and P. Romatschke, Eur. Phys. J. C 75, 15 (2015).
- [33] F. Cooper and G. Frye, Phys. Rev. D 10, 186 (1974).
- [34] H. Grad, Comm. Pure Appl. Math. 2, 331 (1949).
- [35] P. Romatschke, Int. J. Mod. Phys. E 19, 1 (2010).
- [36] R. S. Bhalerao, A. Jaiswal, S. Pal and V. Sreekanth, Phys. Rev. C 89, 054903 (2014).
- [37] P. Staig and E. Shuryak, Phys. Rev. C 84, 034908 (2011).
- [38] E. Shuryak and I. Zahed, Phys. Rev. C 88, 044915 (2013).
- [39] P. F. Kolb, U. W. Heinz, P. Huovinen, K. J. Eskola and K. Tuominen, Nucl. Phys. A 696, 197 (2001).
- [40] V. Roy and A. K. Chaudhuri, Phys. Lett. B 703, 313 (2011).
- [41] B. Abelev et al. [ALICE Collaboration], Phys. Rev. C 88, 044910 (2013).
- [42] E. Retinskaya, M. Luzum and J. Y. Ollitrault, Phys. Rev. C 89, 014902 (2014).
- [43] H. Niemi, G. S. Denicol, H. Holopainen and P. Huovinen, Phys. Rev. C 87, 054901 (2013).
- [44] L. Yan, J. Y. Ollitrault and A. M. Poskanzer, Phys. Lett. B 742, 290 (2015).